OCEANOLOGICA ACTA · VOL. 24 – No. 3

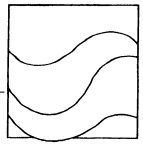

Sorosite (η-Cu_6Sn_5)-bearing native tin and lead assemblage from the Mir zone, Trans-Atlantic Geotraverse hydrothermal field (Mid-Atlantic Ridge, 26°N)

Vesselin M. DEKOV[a]*, Zhelyazko K. DAMYANOV[b], George D. KAMENOV[c], Ivan K. BONEV[d], Istvan RAJTA[e,f], Geoff W. GRIME[e]

[a] Department of Geology and Paleontology, Sofia University, 15 Tzar Osvoboditel Blvd., 1000 Sofia, Bulgaria
[b] Central Laboratory of Mineralogy and Crystallography, Bulgarian Academy of Sciences, 92 Rakovski Str., 1000 Sofia, Bulgaria
[c] Department of Geology, Florida International University, University Park, 11200 Southwest 8th Street, PC 304, Miami, FL 33199, USA
[d] Section of Mineralogy, Geological Institute, Bulgarian Academy of Sciences, bl. 24 Acad. G. Bonchev Str., 1113 Sofia, Bulgaria
[e] Department of Materials, University of Oxford Oxford OX1 3PH, UK
[f] Institute of Nuclear Research of the Hungarian Academy of Sciences, PO Box 51, 4001 Debrecen, Hungary

Received 4 September 2000; revised and accepted 5 December 2000

Abstract − A number of small irregular-shaped and spherical shiny metallic particles have been found in the sediments from the Mir zone, Trans-Atlantic Geotraverse hydrothermal field (Mid-Atlantic Ridge, 26°N). The phase variety of the particles examined is represented by metallic tin, tin-rich lead, and tin–copper phases. A detailed mineralogical study of these particles was carried out using optical microscopy, nuclear microscopy, scanning electron microscopy, electron microprobe, proton microprobe and X-ray diffraction analysis. Tin–lead grains have the typical eutectic microtexture of the metal components. Tin–copper grains are formed from single crystals of sorosite, η-Cu_6Sn_5. The Sn–Pb–Cu complex grains are composed of fine stannoan lead ($Pb_{0.74}Sn_{0.26}$) and tin crystals as well as fine (or occasionally larger) sorosite ($Cu_{6.1}Sn_{4.9}$) idiomorphic crystals, in a tin–lead matrix forming eutectic microtexture. On the basis of data obtained, a natural origin is proposed for the examined Sn–Pb–Cu association, and its parent relations with the tectono-magmatic events in the rift zone. This association has probably been formed (1) during the hydrothermal seepings through the Trans-Atlantic Geotraverse sediment cover, or (2) during the evolution of ridge crest magmatic systems. Crystallisation sequence from an initial melt with falling temperature is: firstly sorosite (Cu_6Sn_5) ($T \leq 380$°C) → crystallisation of tin crystals ($T \leq 227$°C) → crystallisation of Sn–Pb eutectic mixture, composed of tin + stannoan lead ($T \leq 183$°C) → limited tin exsolutions in stannoan lead ($T << 183$°C). Sn–Pb–Cu grains might be present as accessory minerals in the basic rocks of the east rift wall, which have undergone degradation, permitting their deposition into rift valley sediments.

**Correspondence and reprints.*
E-mail address: dekov@gea.uni-sofia.bg (V.M. DEKOV).

S0399178400011397/FLA

Résumé − Association de Sn–Pb–Cu dans les dépôts de la zone hydrothermale de Mir, Geotraverse Trans-Atlantique (dorsale médio-Atlantique, 26°N). De petites particules métalliques brillantes de forme irrégulière et sphérique ont été trouvées dans les dépôts de la zone hydrothermale de Mir (dorsale médio-Atlantique, 26°N). Les particules examinées représentent l'étain métallique, l'étain riche en plomb et l'étain riche en cuivre. Une étude minéralogique détaillée de ces particules a été effectuée en utilisant la microscopie optique, la microscopie nucléaire, le microscope électronique à balayage, la micro-sonde d'électrons, la micro-sonde de protons et la diffraction de rayons X. Les grains étain–plomb présentent une microtexture typique des composants métalliques. Des grains d'étain–cuivre sont formés de cristaux simples de sorosite η-Cu_6Sn_5. Les grains complexes de Sn–Pb–Cu se composent de cristaux fins d'étain–plomb ($Pb_{0.74}Sn_{0.26}$) et d'étain ; les cristaux idiomorphes du sorosite ($Cu_{6.1}Sn_{4.9}$) fin dans une matrice d'étain–plomb formant la microtexture eutectique. Une origine « normale » est proposée pour l'association examinée de Sn–Pb–Cu, et ses relations de parenté avec les événements tectono–magmatiques dans la zone de rift. Cette association a été probablement formée (1) pendant une infiltration hydrothermale par la couverture de dépôt géotraverse trans-Atlantique, ou (2) pendant l'évolution des systèmes magmatiques des dorsales. La succession de cristallisations à partir d'une fusion initiale avec la température en baisse est la suivante : le sorosite (Cu_6Sn_5) ($T \leq 380$°C) → cristallisation des cristaux d'étain ($T \leq 227$°C) → cristallisation du mélange eutectique de Sn–Pb, composé d'étain + étain–plomb ($T \leq 183$°C) → exsolutions limités d'étain dans étain–plomb ($T << 183$°C). Les grains de Sn–Pb–Cu pourraient être présents comme des minéraux accessoires des roches basiques de la paroi est du rift qui ont subi la dégradation, permettant leur dépôt dans les sédiments de la vallée de rift.

hydrothermal field / Mid-Atlantic Ridge / native Sn and Pb / sorosite

zone hydrothermale / dorsale médio-Atlantique / étain et plomb natifs / sorosite

1. INTRODUCTION

Findings of native tin, established mainly in placer materials, have been known for a long time and data for them may be found in the basic references (Hosking, 1974; Ramdohr, 1975). Undoubted native tin in bedrocks has been first found in a calcite–quartz–sulfide association at Nesbitt La Bine Mines (Silman, 1954). More recently, native tin and tin alloys have been described in various types of terrestrial (Ramdohr, 1975; Kovalskii, 1981; Novgorodova, 1994) and lunar (Gay et al., 1970) rocks, and impact materials (Gurov and Kudinova, 1987).

In oceanic environments a wide spectrum of native minerals has been established in the mafic and ultramafic lithologies of the crust (Leinen et al., 1986; Shterenberg et al., 1993; Prichard et al., 1996), metalliferous sediments overlying the basalt basement (Jenkyns, 1976; Marchig et al., 1986), seafloor massive sulfides (Hannington et al., 1986; Zierenberg et al., 1993) and submarine hydrothermal plumes (Jedwab and Boulègue, 1984). Native tin and tin alloys were found in pelagic sediments (Arsamakov et al., 1988), and metalliferous sediments of the Galapagos Rift (Lazur et al., 1989) and East Pacific Rise (Dekov et al., 1996).

We report here the first finding of a ternary sorosite–lead–copper (Sn–Pb–Cu) association in the near sulfide mound sediments of the Trans-Atlantic Geotraverse (TAG) hydrothermal field, Mid-Atlantic Ridge, 26°N.

1.1. Geologic setting

Since the discovery of high-temperature hydrothermal activity in the Mid-Atlantic Ridge (MAR) (Rona et al., 1986), the TAG hydrothermal field (MAR 26°N) has been the classic area for studies of recent hydrothermal discharge and mineralisation on slow-spreading centres. The TAG field, which comprises three sulfide mounds (one active and two dead), has been the focus of a number of studies over the past fifteen years (Campbell et al., 1988; Lisitsyn et al., 1989; Rona et al., 1993; Humphris et al., 1998). In an effort to collect novel data about the tectono-magmatic activity and related events at the TAG field, the 15th cruise of the RV *Akademik Mstislav Keldysh*, with the DSV *Mir-1* and *Mir-2* aboard, took place in the spring of 1988. The results of geophysical, tectonic, and hydrochemical observations, as well as

studies of basement rocks, hydrothermal deposits and rift valley sediment cover have been published (Lisitsyn, 1992).

The TAG hydrothermal field lies on the rift valley floor of the slow-spreading MAR (half rate of accretion 1.1–1.3 cm year^{-1}; McGregor et al., 1977) between the Atlantis (30°40'N) and Kane (24°N) fracture zones (Sempéré et al., 1990) (*figure 1A*). The rift valley is characterised by an asymmetric structure. The east wall is higher and steeper than the west wall (Rona et al., 1986; 1993) and exposes the sheet–dike complex and gabbro layer on its lower part (Lisitsyn, 1992). The active high-temperature sulfide mound is located east of the spreading axis on the rift valley floor. It is a large and steep-sided edifice. The central part consists of a black smoker complex surrounded by a wide platform with a group of white smokers and an apron of metalliferous sediments (Rona et al., 1986; 1993). Two inactive sulfide deposits (named Mir and Alvin) occur on the lower east wall of the rift valley and are undergoing extensive mass-wasting (Lisitsyn et al., 1989; Lisitsyn, 1992; Rona et al., 1993). The Mir relict hydrothermal zone showing various stages of weathering was found in 1988 (Lisitsyn et al., 1989). It is situated between the low-temperature zone, some 300 m higher on the wall (Rona et al., 1984), and the active high-temperature sulfide mound (Rona et al., 1993).

2. MATERIALS AND METHODS

The materials we used in this study were subsamples of a gravity core taken during the 15th cruise of the RV *Akademik Mstislav Keldysh*. The core was collected close to the Mir zone (*figure 1B*). The sediment cover surrounding the Mir mound is composed of nanofossil–foraminiferal and foraminiferal–nanofossil oozes with intercalations of metalliferous sediments and layers rich in basaltic clasts (*figure 1C*). The samples have been hermetically stored at room temperature in polythene boxes (100 mL) since the time of collection. Before analyses all samples were washed with distilled water to remove interstitial salts. The samples were separated into size fractions (> 2.0, 2.0–1.0, 1.0–0.1, 0.1–0.01, 0.01–0.001, < 0.001 mm) by wet sieving in a controlled lab environment (20°C).

The extremely low contents of metallic particles in oceanic sediments (Dekov et al., 1996) prevented the use of routine bulk mineralogical techniques for particle diagnostics. Due to the difficulty to investigate the possible metallic particles from the fine (< 0.10 mm) sediment fractions (Dekov et al., 1996), we examined exclusively the coarse fractions (> 0.10 mm) under a stereomicroscope. Single metallic grains were hand-picked with a steel needle for further mineralogical studies. Preliminary diagnostics of the separated grains was done by means of semi-quantitative energy-dispersion analyses (EDS).

The micromorphology, size and chemical composition (point analyses and area scanning onto polished sections) of the Sn–Pb–Cu specimens were investigated by scanning electron microscope Jeol T-300 with a Link 860-500 EDS and ZAF/PB program, and a Philips SEM-515 with an Edax PV 9100 EDS system (with an operating voltage of 20–25 kV and electron beam diameter of 1 μm). The chemical composition (point analyses) was determined by employing a Cameca microprobe unit (accelerating voltage of 15 kV; beam current of 15 nA; electron beam diameter of 1 μm). The following standards and X-ray lines were used: pure synthetic tin (Sn L_α), pure synthetic copper (Cu K_α) and PbTe (Pb L_α). The detection limits were 0.5% (weight).

Together with the conventional electron microscopy we applied a nuclear microscopy to the analysis of native Sn–(± Pb) – (± Cu) grains. The chemical composition (point analyses) of representative specimens was analysed using the Oxford scanning proton microprobe facility (Grime et al., 1991; beam of 3 MeV protons focused to 1 μm diameter with a current of 100 pA) with a proton induced X-ray emission (PIXE) system and GUPIX program (Maxwell et al., 1995). The highly quantitative PIXE technique (Johansson and Campbell, 1988; an accuracy of 5–10% and a sensitivity in the order of 1–10 ppm) can detect all elements heavier than Na simultaneously. X-rays were detected using a lithium-drifted silicon detector with 70 mm^2 active area positioned at 45° to the beam at a distance of 70 mm. The spatial distribution of different phases within the samples was investigated by scanning the beam over different sized areas (between 750×750 μm^2 and 25×25 μm^2) of the sample and forming PIXE maps of the major elements. The X-ray diffraction patterns of the metallic particles were obtained with a 57.3 mm Gandolfi camera employing Ni-filtered Cu K_α radiation without internal standard (with an operating voltage of 40 kV and a beam current of 19 mA).

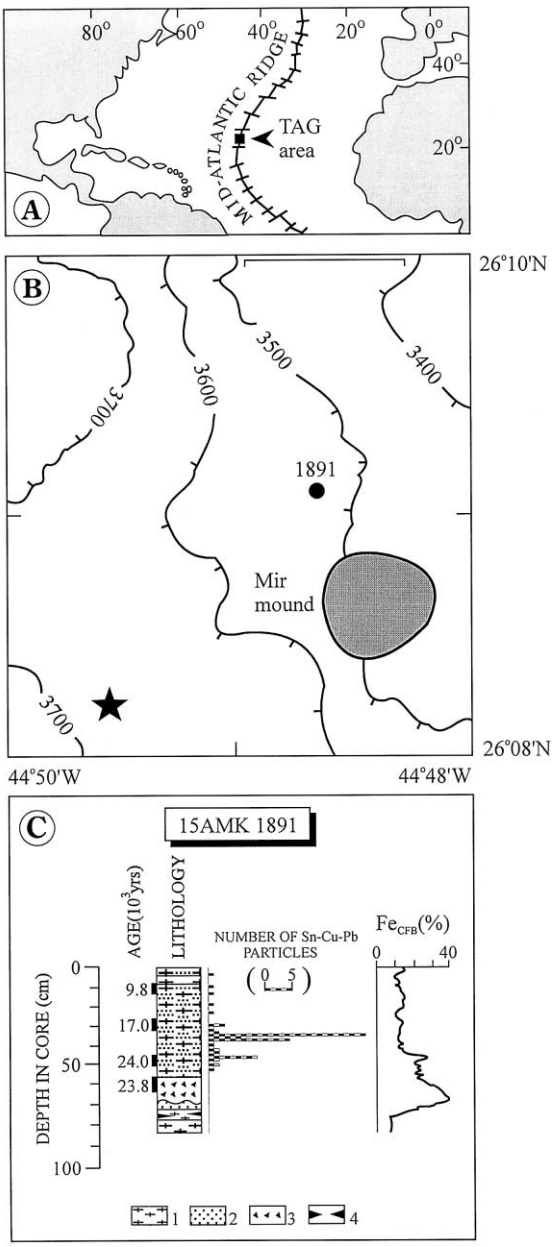

Figure 1. A. Index map showing the location of the Trans-Atlantic Geotraverse area at the Mid-Atlantic Ridge. **B.** Bathymetric map (based on Rona et al., 1993) of the investigated area showing the position of sediment sample station (solid dot), the active high-temperature sulfide mound (star) and the inactive Mir mound (bar in upper right is 1 km long). **C.** Stratigraphic section showing the lithology, number of Sn–Pb–Cu particles found and vertical distribution of the main chemical tracer of hydrothermal activity - Fe (on a carbonate-free basis) in the studied core (based on Lisitsyn et al., 1989). 1 = nanno–foram and foram–nanno oozes; 2 = disseminated hydrothermal component; 3 = clastic sulfide–oxyhydroxide flow; 4 = nontronitic lenses.

3. RESULTS

The EDS analyses of the separated metallic grains (total of 88) have established metallic tin (14% of total grains), tin–lead (48%), tin–copper (12%) and tin–lead–copper (26%) phases. About 80% of total particles found have an irregular shape while the rest 20% are spherical and rounded. Microprobe studies onto polished sections revealed that most of the tin and tin–lead particles contained traces of Cu. This is why we concentrated our investigations on the Sn–Pb–Cu occurrences.

Metallic particles were found to occur along with oxides and hydroxides (chromite, cuprite, tenorite, magnetite, maghemite, hematite, ilmenite, rutile, goethite), sulfides (chalcocite, pyearite, marcasite, chalcopyearite), halogenides (atacamite), sulfates (barite), and silicates (quartz, olivine and plagioclase phenocrysts).

The Sn–Pb–Cu particles are soft, lamella- to irregular-shaped (*figure 2A*), spherical (*figure 2B*) or drop-like, silver-white to grey–white in colour and with metallic lustre. A typical eutectic microtexture (*figure 2C,D*) is observed on the smoothed grain surfaces. Findings of tin (traces of Pb and Cu; *figure 2E*) and needle-like tin–copper (*figure 2F*) crystals at the periphery of the Sn–Pb–Cu particles are fairly rare. Occasionally, the metallic particles are partly covered by a mass of red–brown Fe-oxyhydroxides and coccoliths (*figure 2E,F*). Coatings of secondary oxides, hydroxides and oxychlorides are present on some particles. They are thin, whitish grey, soft and fragile. The bulk (90%) of the Sn–Pb–Cu grains are concentrated in 0.10–0.25 mm fraction.

In reflected light (polished section examinations) the metallic particles are observed to consist almost entirely of a soft, highly reflective, white intergrowth, corresponding to a eutectic texture (*figure 3C*) of platy white pure tin (EDS study) with greyish-white Sn-rich lead. Within this eutectic are observed fine micro-inclusions as well as single brownish–rose 'porphyearitic' crystals of a tin–copper phase. This rose mineral is non-bireflectant in air and oil, and exhibits pronounced anisotropism in oil. Its reflectance is lower than in tin and lead–tin phases. Despite their obvious softness, the tin–lead–copper particles take a good polish, with only a few scratches. The relative hardness of tin–copper crystals is greater than those of tin and lead–tin. The tin–copper crystals much resemble sorosite in their optical properties, appearance as well as associated minerals (native tin and lead).

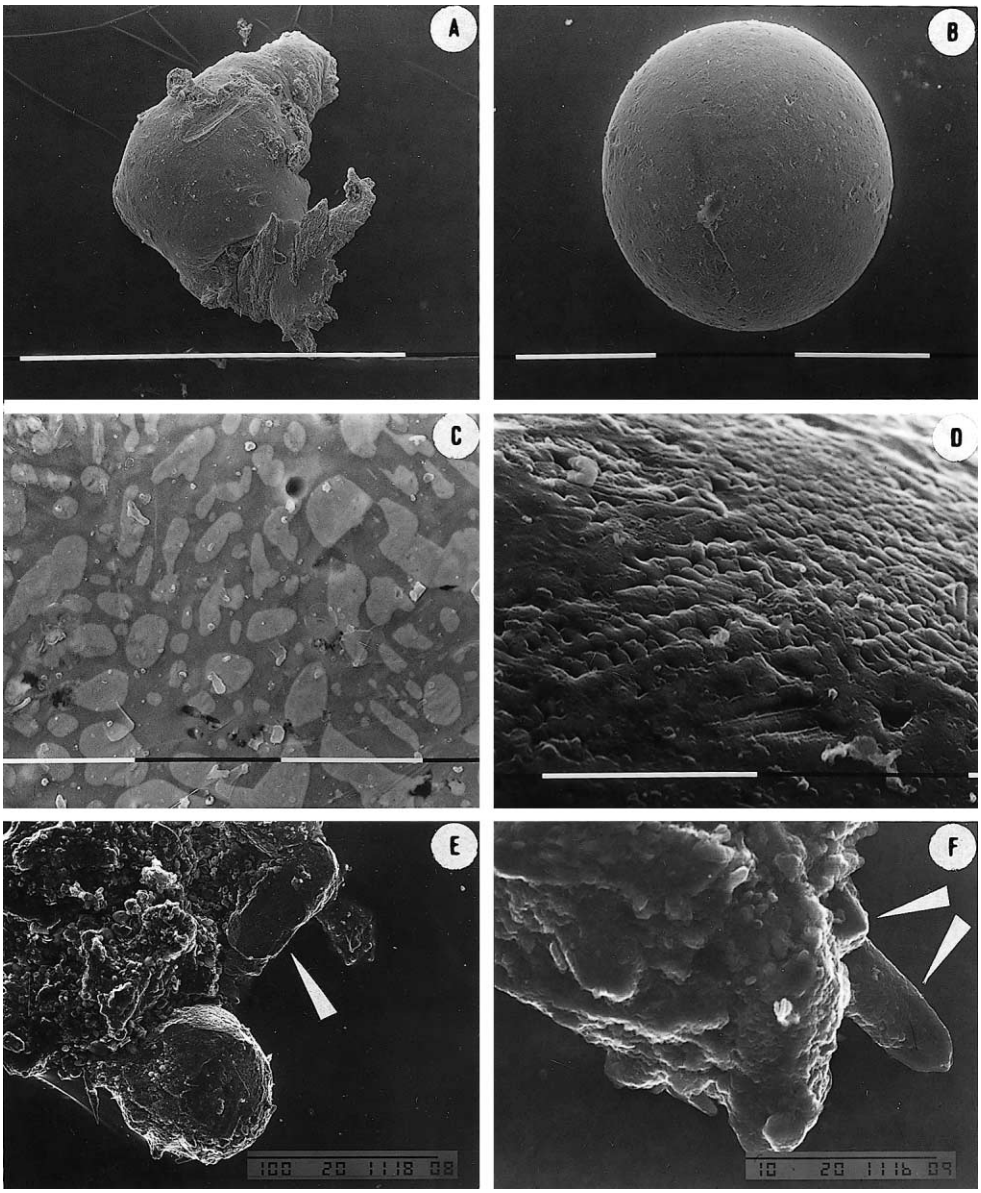

Figure 2. Scanning electron microscope photographs of: **A.** irregular-shaped Sn–Pb–Cu grain (H105I.S48); **B.** spherical Sn–Pb–Cu grain (H105I.S60); **C.** eutectic microtexture of the Sn–Pb–Cu grain shown at (**A**) (enlargement of the central grain surface); lead–tin inclusions (light grey) in a tin matrix (grey); **D.** eutectic microtexture of the Sn–Pb–Cu grain shown at (**B**) (enlargement of the upper grain surface); **E.** tin crystal (arrow) at the periphery of a Sn–Pb–Cu grain (H105II.S40); **F.** tin–copper crystals (arrows) at the periphery of a Sn–Pb–Cu grain (H105II.S12). Scale bars equal to 1000 μm (**A**), 100 μm (**B, E**) and 10 μm (**C–F**).

PIXE mapping of the polished sections (*figure 3*) supports our microscopic observations: the particles studied are composed of fine lead–tin and tin–copper inclusions even distributed within a tin matrix. The tin–copper phases occur as tiny, probably elongated grains (*figure 2F*) and very seldom as bigger idiomorphic crystals of 'porphyearitic' type (*figure 3A,B*). Tin and lead–tin phases are uniformly distributed within the eutectic mixture and the rare tin–copper crystals are notable on that background (*figure 3*).

The lead–tin inclusions in the tin matrix have an uniform composition close to $Pb_{83.5}$,$Sn_{16.5}$ (in percent of the weight, i.e. $Pb_{74.3}Sn_{25.7}$ in percent of atoms) (*table I*) and fairly constant average atomic ratio of $Pb/Sn = 2.9 \pm 0.05$. They have to be defined as stannoan lead, i.e. solid solution of lead with high Sn content in the crystal lattice. Phases with similar compositions have only been found in alluvial placers from the Central Ural Mountains (Aleksandrov, 1955), and basic rocks from the Siberian Platform (Okrugin et al., 1981; see also *table I*).

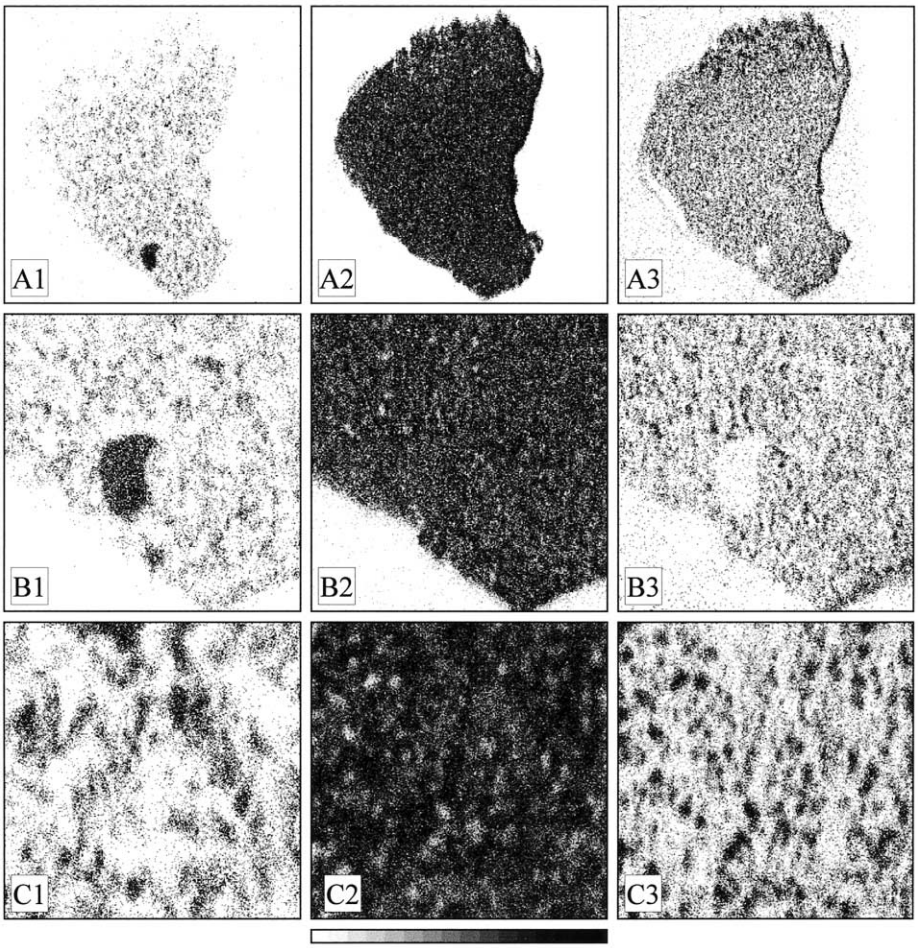

Figure 3. Internal microtextural peculiarities of Sn–Pb–Cu association (H105I.S48). **A.** Cross section of the Sn–Pb–Cu grain. **B.** Tin–copper crystal (η-Cu_6Sn_5-type) in the tin–lead eutectic matrix (enlargement of the lower part of the section shown in (**A**)). **C.** Eutectic texture of the tin–lead matrix with fine tin–copper crystals disseminated (enlargement of the upper-right part of the scan area shown in (**B**)). Proton-induced X-ray emission scans in CuKα (**A1**–**C1**), SnLα (**A2**–**C2**) and PbMα (**A3**–**C3**). Scale bars (lower-right) in μm.

Tin–lead occurrences from the East Pacific Rise metalliferous sediments differ in composition from the TAG Sn–Pb–Cu particles (*table I*).

The composition of tin–copper crystals from the particles studied is also uniform and fairly constant (*table I*). Their average crystallochemical formula is $Cu_{6.1}Sn_{4.9}$, i.e. very close to sorosite (η-Cu_6Sn_5) (Barkov et al., 1998) defined at Baimka placer, despite the relative excess in Cu and the absence of Sb in the composition of the studied crystals. Similar tin–copper phases were also found in gold–platinoid concentrates from southeast Borneo (Stumpfl and Clark, 1965), tin ores from Panasqueira mine, Portugal (Clark, 1972), alluvial heavy mineral concentrates from Rio Tamaná, Colombia (Rose, 1981), some gold–silver deposits in Russia (Gamyanin et al., 1981), and soil and stream sediments from the US Virgin Islands (Alminas et al., 1994; *table I*). We could not perform correct quantitative microprobe analyses on the thin, fragile secondary rind of the particles because of its bad polishing.

Area scanning applied to sections (200 × 200 μm) of the eutectic tin–lead–copper mixture gave the following mean composition (in percent of weight): Sn 76.4 ± 0.9, Pb 16.6 ± 0.05, and Cu 7 ± 0.9 (respectively in percent of atoms: Sn 77.3 ± 1.5, Pb 9.6 ± 0.05, and Cu 13.1 ± 1.5). These data are indicative of the probable composition of the initial melt.

During the semi-quantitative EDS microprobe investigations, some trace elements were detected: Zn (in all types of particles – tin–lead–copper, lead–tin and tin–copper), Fe (in tin–copper particles) and Mn (in one lead–tin grain).

Table I. Chemical composition of native Sn° and Sn–(± Pb)–(± Cu) phases from different natural objects.

Reference	Rudashevskii et al. (1987)		Kovalskii and Oleynikov (1985)										Okrugin et al. (1981)				Glavatskih (1990)			
Object and area of investigation	Ultrabasic rocks, Koryakskoe mountain, Russia		Kimberlite pipes, kimberlite breccia, Yakutiya, Russia		Kimberlite pipes, serpentinized garnet-spinel peridotites, Yakutiya, Russia								Basic rocks, Siberian Platform, Russia				Basalts, Kamchatka, Russia			
Sample No.			OL-55, 44-77		OL-210, 44-75		OL-214, 42-28		OL-214, 45-14		OL-149, 44-46		OB-242-3	OB-54-4D	OL-54-2					
Phase	tin	lead	tin	lead	tin	lead	Cu_6Sn_5-type	Cu_3Sn-type	tin	Cu_6Sn_5-type	tin	Cu_6Sn_5-type	tin	tin	lead	tin	lead	tin	lead	tin
Sn	99.00	1.97	96.14	2.04	100.58	2.46	61.09	42.16	98.30	65.72	99.19	66.10	97.11	95.99	15.93	92.89	0.53	94.27	0.30	96.75
Pb	1.27	96.30	2.39	95.77	0.21	98.41	–	1.46	0.25	1.64	0.27	0.16	0.48	3.78	85.53	4.22	99.42	–	99.96	–
Cu	–	–	–	–	0.06	0.08	37.68	54.51	0.30	34.01	0.24	33.87	–	–	–	–	–	–	–	–
Zn	–	–	–	–	–	–	–	–	–	–	–	–	–	–	–	–	–	–	–	–
Sb	–	–	0.51	–	–	–	–	–	–	–	–	–	2.01	0.13	0.13	2.31	–	4.73	–	3.26
Total	100.27	98.27	99.04	97.81	100.85	100.95	98.77	98.13	98.85	101.37	99.70	100.13	99.60	99.90	101.59	99.42	99.95	99.00	100.26	100.01

Reference	Gamyanin et al. (1981)		Ippatyeva (1981)	Lazur et al. (1988)			Gurov and Kudinova (1987)		Rose (1981)	Clark (1972)		Kucha (1981)	Lawrence (1951)
Object and area of investigation	Granitoids, South-Verkhoyanskii synclinorium, Russia		Granitoids, Maastakhskii intrusive, Russia	Sandstones, clay shales and diabases, Ural, Russia			Impact material, meteoritic crater Elgygytgyn, Russia		Alluvial heavy mineral concentrates, Rio Tamaná, Colombia	Tin ores, Panasqueira Mine, Portugal		Zechstein copper deposits, Lubin Mine, Poland	Alluvial placers, Emmaville, NSW, Australia
Phase	Cu_6Sn_5-type		tin	tin			Sn-Pb-Cu		Sb-bearing η-Cu_6Sn_5	η'-Cu_6Sn_5		lead	tin
Sn	67.70	66.60	99.00	99.60	63.76	63.34	63.00	67.00	56.12	61.10	61.20	–	95–97
Pb	–	–	–	–	–	–	35.00	30.00	–	–	–	100.00	traces
Cu	32.30	33.40	–	–	36.14	36.98	0.30	0.30	35.99	38.70	38.50	–	–
Zn	–	–	1.60	–	–	–	–	–	–	–	–	–	–
Sb	–	–	–	–	–	–	–	–	7.89	–	–	–	–
Total	100.00	100.00	100.60	99.60	99.90	100.32	98.30	97.30	100.00	99.80	99.70	100.00	95–97

Table I. Continued.

Reference	Burke and Dunn (1988)	Alminas et al. (1994)								Barkov et al. (1998)						
Object and area of investigation	Ores, Franklin mine, USA	Soil and stream-sediments, US Virgin Islands, Greater Antilles Island arc								Gold placer deposit, Baimka River, western Chukotka, Russian Far East						
Sample No.	NMNH # C6061-1	SC514A	SJ601A	SC514	SJ601	29	10C	10D	SJ738-2-16	1	2	3	4	5	6	9
Phase	lead	tin	lead	lead	lead	lead	Cu_6Sn_5	Cu_6Sn_5	Cu_6Sn_5	sorosite	sorosite	sorosite	sorosite	sorosite	sorosite	tin
Sn	–	99.6	0.0	6.0	0.2	0.0	61.5	61.1	61.1	57.99	58.18	56.78	62.59	62.98	62.49	98.17
Pb	99.5	0.3	100.6	94.6	99.7	101.0	–	–	–	–	–	–	–	–	–	–
Cu	–	–	–	–	–	–	38.4	38.2	38.2	36.12	35.33	35.96	36.45	36.88	36.92	–
Ni	–	–	–	–	–	–	0.0	0.3	0.6	–	–	–	–	–	–	–
Fe	–	–	–	–	–	–	–	–	–	0.92	1.18	1.26	–	–	–	–
Sb	–	–	–	–	–	–	–	–	–	4.93	4.77	4.89	0.91	0.87	1.11	1.71
Total	99.5	99.9	100.6	100.6	99.9	101.0	99.9	99.6	99.9	99.96	99.46	99.53	99.95	100.73	100.52	99.88

Reference	Dekov et al. (1996)							Present study							
Object and area of investigation	Metalliferous sediments, EPR 21°S							Hydrothermal sediments, Mir mound, TAG field, MAR 26°N							
Sample No.	H2.S6		H22.S10					H105I.S48							
Phase	tin	copper	tin	lead	tin	lead	tin	Cu_6Sn_5-type	Cu_6Sn_5-type	Cu_6Sn_5-type	Cu_6Sn_5-type	Cu_6Sn_5-type	lead-tin	lead-tin	tin
Sn	97.61	5.55	99.21	5.15	97.49	7.51	99.27	59.98	59.65	59.29	59.13	59.82	16.73	16.47	98.43
Pb	–	–	0.79	94.27	2.41	91.61	0.51	–	–	–	–	–	83.27	84.55	–
Cu	0.33	79.16	–	0.03	0.10	0.09	0.22	39.68	39.96	39.82	40.46	40.13	–	–	–
Zn	–	–	–	–	–	0.19	–	–	–	–	–	–	–	–	–
Fe	–	0.13	–	–	–	–	–	–	–	–	–	–	–	–	–
Ti	0.54	0.31	–	–	–	–	–	–	–	–	–	–	–	–	–
Al	1.52	14.86	–	0.54	–	0.60	–	–	–	–	–	–	–	–	–
Total	100.00	100.01	100.00	99.99	100.00	100.00	100.00	99.66	99.61	99.11	99.59	99.95	100.00	101.02	98.43

Values are in percent of weight.

All reflections typical for Sn_{syn} and Pb_{syn} were established on the X-ray diffraction (XRD) pattern of the Sn–Pb–Cu phase (*table II*). Basic reflections of sorosite or its synthetic equivalent η-$Cu_{6.26}Sn_5$ (PDF # 47-1575) were absent on the XRD pattern, although such a phase was undoubtedly identified by microprobe analyses in the particle studied. This could be due to relatively low content of the tin–copper crystals in the specimen examined and the close proximity of η-$Cu_{6.26}Sn_5$ standard basic lines (2.9640 Å (101), 2.1030 Å (110) and 2.0886 Å (102)) with those of the obtained pattern (2.92 Å (I = 6) and 2.06 Å (I = 3); *table II*). There is, however, a coincidence of some minor XRD peaks of the studied phase (indexed as Sn° and Pb° peaks) with those of sorosite (*table II*). The XRD patterns of previously studied tin–lead particles from the metalliferous sediments from the EPR 21°S suggest that these phases probably contain sorosite too (*table II*).

Estimated cell parameters of the tin phase are practically identical with the standard ones (*table II*). In contrast, the measured a_{Pb} = 4.947 Å is less than the pure standard one (a_{Pb} = 4.9506 Å; PDF # 4-686) (*table II*). This is obviously a result of the inserting through solid solution of Sn atoms (with atomic radius (1.58 Å) smaller than Pb (1.75 Å)) into the Pb cell.

4. DISCUSSION

4.1. Genesis of the Sn–Pb–Cu association

The occurrence of a large proportion of unorthodox native metals (other than noble Au^o, Ag^o and platinum group elements) and alloys had long been regarded as sampling artefacts. Indeed, it is difficult to understand how elements generally combined with oxygen or sulfur could exist in a metallic state in Nature, although a number of papers on this matter have been published during the past years (summarised by Ramdohr, 1975; Kovalskii, 1981; Novgorodova, 1994; etc.). We are well aware of the possibility that metallic occurrences found in the TAG sediments may be anthropogenic. In our previous works on native metals in oceanic hydrothermal sediments (Dekov et al., 1996; Dekov et al., 1999) we discussed the possibility of the technogenic nature of these occurrences. Here we will add some additional facts that lend support to the idea of the natural origin of studied particles:

– The probable initial melt composition of the investigated particles ($Sn_{76}Pb_{17}Cu_7$; weight percentage) differs from that of anthropogenic Sn–Pb systems. The most typical tin–lead solders are predominantly Sb-bearing. Some special types of solders contain up to 1.5% of Cu (weight) (for example: LSn60Cu1.5 - TGL 14908 standard; Neumann and Richter, 1979), while in the present case, the Cu content is considerably greater (*table I*). The material from tin–lead artefacts typically contain 100 ppm or more silver together with alumina spheres, while the natural material does not (Alminas et al., 1994). It is also indicative the fact that alloys with similar compositions have been less favourable objects of investigation during the study of the ternary Sn–Pb–Cu system (see data summarised by Chang et al., 1979; Marcotte and Schroder, 1983);

– The close association of a great number of Sn–Pb–Cu particles with native nickel, native copper and copper–zinc alloys which are characteristic for some oceanic sediments (Shterenberg, 1993) and continental ultrabasic and basic rocks (Kovalskii, 1981; Novgorodova, 1994). The association of the Sn–Pb–Cu particles with typical hydrothermal and basaltic minerals;

– The bulk of particles were found in core samples from sediment layers formed in pretechnogenic times (older than 9.10^3 years) (*figure 1C*). There are no data (radiocarbon, geochemical, lithologic, biostratigraphic) supporting resedimentation of the materials studied.

The facts discussed above and our previous investigations (Dekov et al., 1996; Dekov et al., 1999) favour a natural origin for the Sn–Pb–Cu particles from the TAG sediments. Different hypotheses may explain the natural origin of the studied particles:

– Fluvial origin. The remoteness of the studied area from the landmasses, and relatively high specific gravity of the Sn–Pb–Cu particles suggest that a fluvial origin of these metallic grains is unlikely.

– Aeolian origin. Eastern winds from the Sahara desert carry a lot of terrestrial dust to the Central Atlantic (Lisitsyn, 1972). Extensive alteration of the shape of the aerosol particles during transport in dust clouds forms typical surface microtextures that we have not observed. We think that the aeolian origin of studied particles is also not possible.

– Meteoritic origin. As a rule, volatile metals such as tin and lead are depleted in extraterrestrial matter (Mason and Melson, 1970). Meteorites burning during their passage through the atmosphere could not generate mi-

Table II. X-ray diffraction data for native Sn° and Sn–(± Pb)–(± Cu) phases from different natural objects.

Reference	Present study		Dekov et al. (1996)				Butuzova et al. (1987)		Okrugin et al. (1981)		Gurov and Kudinova (1987)		Tomson et al. (1989)		Barkov et al. (1998)		PDF							
Object and area of investiga-tion	Hydrothermal sediments, Mir mound, TAG field, MAR 26°N		Metalliferous sediments, EPR 21°S				Metalliferous sediments, Atlantis-II Deep, Red Sea		Basic rocks, Siberian Platform, Russia		Impact material, meteoritic crater Elgygytgyn, Russia		Graphite-ilmenite metasomatites, Kavalerovo district, Primorie, Russia		Gold placer deposit, Baimka River, western Chukotka, Russian Far East								
Metallic phases	Sn–Pb–Cu		Native Sn°		Sn–Pb		Pb–Sn		Sn–Pb		Sn–Pb–Cu		Sn–Pb		sorosite		Sn_{syn}			Pb_{syn}			η-$Cu_{6.26}Sn_5$	
Sample No.	H105I.S48		H23.S27		H22.S10		–		OB-54-4b		–		–		–		# 4-673			# 4-686			# 47-1575	
Analytical conditions																								
Radiation	Cu K_α		Cu K_α		Cu K_α		Co K_α		Fe $K_{\alpha,\beta}$		Cu K_α		–		Fe K_α		Cu K_α			Cu K_α			Cu K_α	
Filter	Ni		Ni		Ni		–		–		–		–		–		Ni			Ni			Ni	
U (kV)	40		40		40		–		–		–		–		–		–			–			–	
I (mA)	19		19		19		–		–		–		–		–		–			–			–	
Exposition time (h)	25.05		35		40		5–6		–		–		–		–		–			–			–	
Camera	57.3 mm Gandolfi		57.3 mm Gandolfi				57.3 mm Debye-Scherrer		57.3 mm Debye-Scherrer		57.3 mm Debye-Scherrer		–		114.6 mm Debye-Scherrer		–			–			Diffractometer	
Results	*I**	*d* (Å)	I	*d* (Å)	I	*d* (Å)	I	*d* (Å)	I	*d* (Å)	I	*d* (Å)	I	*d* (Å)	I	*d* (Å)	I	*d*(Å)	*hkl*	I	*d* (Å)	*hkl*	I	*d* (Å)	*hkl*
					10	2.95(s)									10	2.970									
	6	2.92	10	2.92			10	2.89	2	2.914	3	2.902	10	2.920			100	2.915	200						
	9	2.85			10	2.86			3	2.857	6	2.849	10	2.860						100	2.855	111			
	9	2.78	10	2.77	10	2.79			4	2.789	3	2.780	10	2.792			90	2.793	101						
					1	2.62																			
															1	2.560							5	2.5489	002
	5	2.44			8	2.48	4	2.49	4	2.476	5	2.452	7	2.484						50	2.475	200			
															8	2.112							82	2.1030	110
															9	2.094							64	2.0886	102
	3	2.06	5	2.05	4	2.06			2	2.060	2	2.058					34	2.062	220						
	8	2.01	10	2.00	10	2.01	2	2.02	5	2.017	4	2.010	9	2.000			74	2.017	211						
	7	1.746			5	1.746	3	1.75	4	1.752	4	1.746	8	1.752						31	1.750	220			
															3	1.720							18	1.7153	201
	3	1.658	4	1.652	3	1.663			2	1.661	3	1.661					17	1.659	301						
															2	1.627							8	1.6222	112
															2	1.546							10	1.5399	103
	10	1.492			8	1.488	5	1.49	10	1.492	10	1.490	10	1.493						32	1.493	311			
	10	1.484(s)	4	1.479(s)											5	1.487	23	1.484	112				20	1.4819	202
	1	1.457	2	1.450	1	1.454					1	1.451					13	1.458	400						
	2	1.441	4	1.434	3	1.442			3	1.442	1	1.443					20	1.442	321						
	1	1.427					2	1.43	2	1.426	1	1.431								9	1.429	222			
					1	1.357(s)			1	1.328					4	1.333							4	1.3291	211

Table II. Continued.

	2	1.305	3	1.302	2	1.308			3	1.305	1	1.305					15	1.304	420					
	2	1.293	3	1.289	2	1.296			4	1.295	1	1.296					15	1.292	411					
															2	1.279						3	1.2742	004
	1	1.238(s)							2	1.237	1	1.238			1	1.248				2	1.236	400	4	1.2423	203
					5	1.217									5	1.218							10	1.2142	300
	4	1.204(s)	8	1.201(s)					7	1.207	4	1.207	5	1.204	5	1.212	20	1.205	312				16	1.2112	212
	3	1.135			2	1.132	1	1.13	5	1.137	4	1.137	10	1.134						10	1.1359	331			
	3	1.106			2	1.105			4	1.107	2	1.107	9	1.105						7	1.1069	420			
	3	1.096(s)	3	1.092(s)	2	1.095(s)			3	1.096	1	1.100	3	1.095	4	1.095	13	1.095	431				2	1.0961	302
																							10	1.0898	114
															2	1.072							5	1.0697	213
							2	1.06	1	1.046					2	1.054							7	1.0515	220
									4	1.043	1	1.044					3	1.0434	103						
	2	1.040	2	1.040	1	1.040											5	1.0401	332						
									1	1.034							2	1.0309	440						
	1	1.025	1	1.024	1	1.027			4	1.028	1	1.027					5	1.0252	521						
	3	1.011			1	1.010			6	1.011	1	1.011	10	1.010						6	1.0105	422			
																							4	0.9910	311
	1	0.983(s)	1	0.980(s)	1	0.985(s)			5	0.984							5	0.9824	213				2	0.9818	105
	1	0.972(s)											3	0.972			2	0.9718	600				2	0.9721	222
	3	0.953			1	0.945					3	0.955								5	0.9526	511			
																							8	0.9392	312
											2	0.931					3	0.9310	303						
	3	0.929	2	0.927	2	0.929											13	0.9286	512						
	1	0.922															5	0.9219	620						
	1	0.917	1	0.916													5	0.9178	611						
																							2	0.8965	401
	1	0.887(s)	2	0.886(s)													4	0.8868	323				1	0.8896	205
	3	0.876(s)	3	0.875(s)													2	0.8755	541	1	0.8752	440	6	0.8791	304
																							3	0.8684	313
																							3	0.8576	402
	5	0.848															4	0.8485	413						
			5	0.846													10	0.8466	532						
	1	0.839	3	0.838													4	0.8386	631						
	5	0.836																		9	0.8369	531			
																							3	0.8274	106
	2	0.825(s)																		4	0.8251	600	4	0.8247	321
																							3	0.8193	215
																							8	0.8111	224
	1	0.809	2	0.808													6	0.8086	640						
	1	0.806	1	0.806													3	0.8058	701						
																							3	0.8027	403
a_{Sn} (Å)	5.833 (4)		5.82		5.84				5.84		5.831		5.83				5.831								
c_{Sn} (Å)	3.183 (9)		3.17		3.19				3.20		3.182		3.18				3.182								
a_{Pb} (Å)	4.947 (5)				4.95		4.95		4.95		4.951		4.95							4.9506					
$a_{sorosite}$ (Å)															4.217 (4)								4.2062 (1)		
$c_{sorosite}$ (Å)															5.120 (6)								5.0974 (1)		

* Intensities estimated visually. (s): XRD peaks close to sorosite peaks

crospherules with Sn–Pb composition. Cosmic metallic droplets found in the deep-sea sediments consist mainly of Fe and Ni (Blanchard et al., 1980; Brownlee et al., 1997). Particles quite similar in composition (*table I*), shape and size have been found in impact materials of the El'gygytgyn meteoritic crater (Gurov and Kudinova, 1987). The origin of these microspherules has been attributed to the impact process: condensation of a high-temperature gas phase mobilised from the land target under reducing conditions realised during the impact. In the case of open ocean, the target for meteoritic falls could be the oceanic surface and similar processes of Sn–Pb mobilisation and condensation are hardly possible. That is why we believe that an extraterrestrial or impact origin of examined particles has also to be rejected.

– Probable hydrothermal or magmatic origin. We suggest the major factors controlling the Sn–Pb–Cu phase occurrences appear to be the hydrothermal activity and magmatic processes in the TAG rift valley. Most probably these metallic particles have been formed in the hydrothermal sediments themselves and/or have been presented as accessory minerals disseminated in the basic rocks exposed at the foot of high-elevated east rift wall. During bedrock degradation the metallic grains could have been liberated and, in turn, deposited into adjacent sediments.

• Formation related to hydrothermal processes. We consider that the high-temperature hydrothermal discharge at the TAG field have not played a role in the formation of the studied particles. The high activity of reduced sulfur in the TAG hydrothermal vents (Campbell et al., 1988) would provide a sink for chalcophiles (Pb, Cu, Sn) deposited as sulfides rather than their deposition in zero-valent state. Nevertheless, it is known that laboratory synthesis studies (Alminas et al., 1994) in which Pb- and Sn-rich saline solutions were introduced into a $CaCO_3$-rich environment at 25°C, 1 atm and low pH, produced native tin. Metallic particles very similar in composition, shape and size, and in the same mineral associations have been found in the soils and stream sediments of the US Virgin Islands (Alminas et al., 1994). Their origin was attributed to the interaction between metal-rich chloride hydrothermal solutions and calcareous oozes into which the solutions had been injected (Alminas et al., 1994). Seepage of hot hydrothermal fluids through the TAG sediment cover could cause boiling and phase separation (vapor and liquid) of the fluid as in the sediment hosted submarine hydrothermal environments. The low temperature, saline, metal-rich and exhausted in H_2S residual liquid would interact with the calcareous matrix of the TAG oozes and might have precipitated native Sn–Pb–Cu association within the sediment cover.

• Formation in the oceanic crust during the magmatic crystallisation. There are two possible pathways: (1) formation from an immiscible metal liquid during crystal–liquid fractionation processes in magmatic melt; and (2) reduction and crystallisation from a silicate melt matrix. We have already discussed these two models (Dekov et al., 1996) and would like to give attention to some features of the second mode of formation. Experimental studies on the interaction of hydrogen with basic magmatic melts (Persikov et al., 1986) revealed that during these processes Pb, Fe, Ni and Co had been separated as metallic microspherules and irregular-shaped particles in the silicate matrix. We consider that beneath the rift zones with high intratelluric H_2 flux similar processes of metallisation of the peridotitic upper mantle, which partially melts to produce MORB, could occur.

Sorosite-bearing assemblage of native tin and lead in the Baimka placer (Barkov et al., 1998) occurs in an environment, which contains widespread ophiolitic rocks. This implies that metallic Sn–Pb–Cu phases could derive from the mafic and serpentinised ultramafic lithologies of the ancient and recent oceanic crust.

4.2. Formation conditions and sequence of crystallisation

The phase diagrams of the binary systems Cu–Sn and Sn–Pb (after Hansen and Anderko, 1958; Champion et al., 1981) are given in *figure 4*. The Cu–Pb system is monotectic with a eutectic reaction near the high Pb corner. It is not discussed hereafter since the crystallisation pathway of the studied particles does not pass through the Cu–Pb field. The Pb–Sn system shows a simple eutectic, while the Cu–Sn one is more complicated with binary phases and peritectic transformations. The ternary Cu–Pb–Sn system has been studied by Marcotte and Schroder (1983). These authors established the reduction of the decomposition temperature of η-Cu_6Sn_5 with addition of Pb in the Sn–Cu system and a ternary eutectic reaction near the binary Pb–Sn eutectic.

On the basis of the observed microtextural relationships, and phase compositions of the particles examined, the

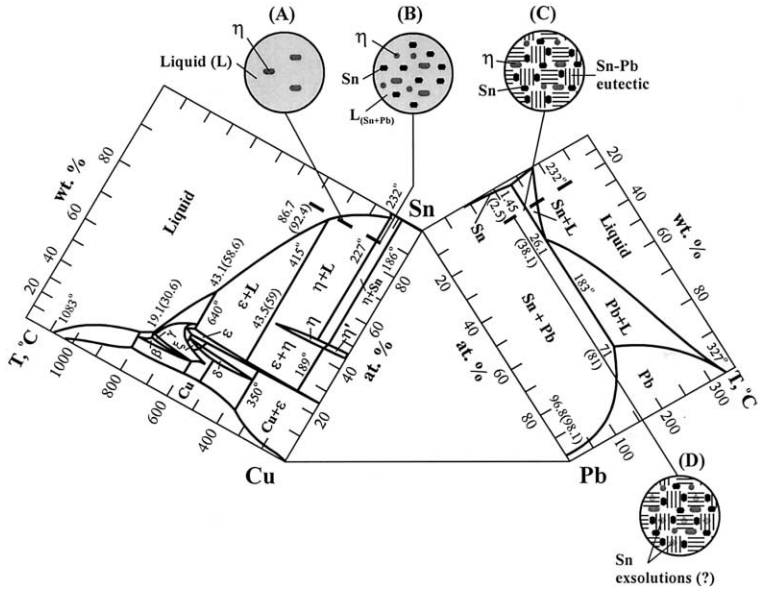

Figure 4. Diagrams of equilibrium of Cu–Sn, Sn–Pb and Cu–Pb binary systems (after Hansen and Anderko, 1958; Champion et al., 1981) and proposed phase variety and microtextural relationships at different solidification stages of the initial ternary Sn–Pb–Cu melt (see explanation in the text).

formation of the Sn–Pb–Cu particles from the TAG metalliferous sediments was probably realised with falling temperature in the following sequence (*figure 4*):

– Crystallisation of sorosite (η-Cu_6Sn_5) from the parent melt (L) at around 380°C. Metallic melt becomes practically exhausted in Cu. The temperature, experimentally found by Marcotte and Schroder (1983) as a η-Cu_6Sn_5 decomposition temperature of $Sn_{70}Pb_{20}Cu_{10}$ system, was 35°C lower than the one given in *figure 4* because of the Pb addition in the system. The single large ('porphyearitic') η-Cu_6Sn_5 crystals on the background of the fine microcrystalline structure are probably due to gravity segregation.

– Formation of tin crystals from liquid with tentative composition $Sn_{80}Pb_{20}$ started at $T < 227$°C.

– Sn–Pb eutectic, composed of intimate intergrowths of Sn and (Pb,Sn), formed from the remainder liquid at $T < 183$°C and the whole of the melt transformed into solid state. It is well known that Pb at 183°C and under ambient pressure is able to insert up to 29% of Sn atoms in its crystal lattice without changing the crystal structure. This value at 0°C is respectively 3.2% of Sn atoms (*figure 4*). The lead–tin phase ($Pb_{74.3}Sn_{25.7}$ in percent atoms) in the particles studied has Sn content close to the uppermost limit, which may be explained by three different ways:

• very rapid melt cooling (quenching effect) to below the temperature of eutectic crystallisation of the Sn–Pb system (i.e., < 183°C); in this case, such a rapid cooling should prevent appearance of Sn exsolutions within the lead–tin inclusions and the system should remain under non-equilibrium state, in comparison with the low temperature of the parent rock;

• the compositions of the lead–tin inclusions (*table I*) have been obtained from non homogeneous sections including also Sn microexsolutions, this could lead to an overestimation of the actual Sn content during the microprobe investigations (analytical artefact); some non homogeneity of these inclusions can be observed in *figure 2C* and *figure 3C2*;

• the Sn–Pb phase diagram (*figure 4*), gives only a tentative notion of the probable development of the geological processes which takes into consideration one basic physicochemical parameter, the temperature; the behaviour of a melt under high pressures of the magmatogenic mineral-forming processes is not known although the influence of low pressures on the phase equilibrium and crystallisation pathways of metallic systems in liquid and solid state is generally insignificant.

We suppose that in the present case some quantity of tin exsolutions has been separated from the lead–tin solid solution as the temperature falls to below the eutectic level. It is quite possible that this process had not been fully completed and at a certain moment sudden cooling provoked by various geological reasons (for example, opening of the system caused by tectonic movements, mixing with low-temperature igneous derivatives, etc.)

took place. The eutectic microtexture and spherical shape of some of the Sn–Pb–Cu particles studied (*figure 2B,D*) support such a conclusion.

– Sn exsolutions were separated from the lead–tin phase ($Pb_{74.3}$,$Sn_{25.7}$); shortly afterwards sudden cooling of the system stopped the exsolution process giving the association its end phase composition.

The influence of the cooling rate and related diffusion in the system on the microtextural and phase characteristics of the Cu–Sn association in solid state has been established by Champion et al. (1981). Using the explanations of these authors, we may conclude that, as a whole, the investigated Sn–Pb–Cu association might have been formed as a result of relatively rapid cooling of parent melt. This led to an appearance of numerous nuclei creating eutectic and dendrite microtextures of intimate intergrowths of the main solid phases (*figure 2C,D*). The presence of large 'porphyearitic' inclusions of sorosite (η-Cu_6Sn_5), however, testifies to relatively low cooling rate during the initial stage of peritectic reaction (A) when gravity segregation takes place.

5. CONCLUSION

The examined metallic particles of the Sn–Pb–Cu system found in the sediments from the Mir zone, TAG hydrothermal field (Mid-Atlantic Ridge, 26°N) are thought to have a natural origin related to either: 1) the hydrothermal seeping processes in the sediment cover; or 2) formation of rift valley igneous rocks. On the one hand, metal-rich hydrothermal fluids could seep through the TAG sediment cover, react with the calcareous matrix and precipitate tin–lead based metallic particles. On the other hand, Sn–Pb–Cu metallic microsegregations could have been formed magmatically during the evolution of ridge crest magmatic systems: either from an immiscible metal liquid; or by reduction from the silicate melt. The pathway of formation of the Sn–Pb–Cu association and crystallisation kinetics of the process have probably been as follows: relatively slow crystallisation and gravity segregation of sorosite (η-Cu_6Sn_5) at the initial stage of solidification under moderate fall in temperature below 380°C → rapid crystallisation at the middle and final stage of η-Cu_6Sn_5 formation as well as during the Sn–Pb eutectic reaction creating a mixture of tin and stannoan lead (total range of 300°?~183°C) → rapid cooling at T << 183°C (?) stopping the process of tin exsolution.

Magmatic intrusions in the ridge axial zone might have transported the Sn–Pb–Cu segregations within the silicate matrix to the upper earth's crust levels. During the processes of rift valley formation (Lisitsyn, 1992) the gabbro and sheet–dike layers have been exposed and have undergone active disintegration. The native Sn–Pb–Cu grains liberated together with other rock shards have been dispersed into the rift valley sediments.

Special thanks go to: A.P. Lisitsyn, V.M. Kuptsov, and V.V. Serova (all from the Institute of Oceanology, Russian Academy of Sciences) for providing the sediment samples, radiocarbon age dating and preparing lithologic description, respectively; D. Ackermand (Institute of Mineralogy and Petrology, University of Kiel, Germany) for the excellent Cameca microprobe analyses; J. Jedwab (Laboratoire de géochimie, Université libre de Bruxelles, Belgium) and two anonymous reviewers for the helpful suggestions. The financial support given to the authors from Bulgaria by the Bulgarian National Science Foundation (grant NZ-420) is gratefully acknowledged. V.M. Dekov was supported in part through a post-doctoral fellowship from the German Service for Academic Exchange.

REFERENCES

Aleksandrov, A.I., 1955. Native tin in alluvial placers from the Is river (Central Ural Mts.). Zapiski Vsesoyuznogo Mineralogicheskogo Obshchestva (Reports of All-union Mineralogical Society) 84, 462–464 (in Russian).

Alminas, H.V., Foord, E.E., Tucker, R.E., 1994. Geochemistry, mineralogy, and geochronology of the U.S. Virgin Islands. U.S. Geological Survey Bulletin No.2057, pp. 1–36.

Arsamakov, H.I., Kruglyakov, V.V., Marushkin, A.I., 1988. Native metals and alloys in the pelagic sediments of the Pacific Ocean. Litologiya i Poleznye Iskopaemye (Lithology and Mineral Resources) 4, 122–126 (in Russian).

Barkov, A.Y., Laajoki, K.V.O., Gornostayev, S.S., Pakhomovskii, Y.A., Men'shikov, Y.P., 1998. Sorosite, Cu(Sn,Sb), a new mineral from the Baimka placer deposit, western Chukotka, Russian Far East. Am. Mineral. 83, 901–906.

Blanchard, M.B., Brownlee, D.E., Bunch, T.E., Hodge, P.W., Kyte, F.T., 1980. Meteoroid ablation spheres from deep-sea sediments. Earth Planet. Sci. Lett. 46, 178–190.

Brownlee, D.E., Bates, B., Schramm, L., 1997. The elemental composition of stony cosmic spherules. Meteor. Planet. Sci. 32, 157–175.

Burke, E.A.J., Dunn, P.J., 1988. Cuprostibite, domeykite, native copper and native lead from the Franklin Mine, New Jersey (USA). Neues Jahrbuch für Mineralogie, Monahtchefte 4, 145–148.

Butuzova, G.Y., Shterenberg, L.E., Voronin, B.I., Korina, E.A., 1987. Native metals in the Red Sea metalliferous sediments.. Litologiya i Poleznye Iskopaemye (Lithology and Mineral Resources) 2, 122–125 (in Russian).

Campbell, A.C., Palmer, M.R., Klinkhammer, G.P., Bowers, T.S., Edmond,, J.M., Lawrence, J.R., Casey, J.F., Thompson, G., Humphris, S., Rona, P., Karson, J.A., 1988. Chemistry of hot springs on the Mid-Atlantic Ridge. Nature 335, 514–519.

Champion, P., Guillet, L., Poupeau, Ph., 1981. Diagrammes de phases des matériaux cristallins. Masson, Paris.

Chang, Y.A., Neumann, J.P., Mekula, A., Goldberg, D., 1979. The metallurgy of copper. Phase diagrams and thermodynamic properties of ternary copper–metal systems. INCRA Monograph 6, 631–642.

Clark, A.H., 1972. A copper–tin alloy (η'-Cu_6Sn_5) from Panasqueira, Portugal. Neues Jahrbuch für Mineralogie, Monahtchefte 3, 108–111.

Dekov, V.M., Damyanov, Z.K., Kamenov, G.D., Bonev, I.K., Bogdanov, K.B, 1999. Native copper and α-copper-zinc in sediments from the TAG hydrothermal field (Mid-Atlantic Ridge, 26°N): nature and origin. Mar. Geol. 161, 229–245.

Dekov, V.M., Damyanov, Z.K., Mandova, E.D., 1996. Native tin and tin alloys from axial metalliferous sediments of an ultra-fast spreading centre: East Pacific Rise, 21°S survey area. Neues Jahrbuch für Mineralogie, Monahtchefte 9, 385–405.

Gamyanin, G.N., Polovinkin, V.L., Leskova, N.V., 1981. Native metals and intermetals in the granitoids from the North-Eastern USSR ore structures. In: Kovalskii, V.V. (Ed.), Samorodnoe mineraloobrazovanie v magmaticheskom processe (Native mineral formation in the magmatic processes). Yakutsk, 167–172 (in Russian).

Gay, P., Bancroft, G.M., Bown, M.G., 1970. Diffraction and Mössbauer studies of minerals from lunar soils and rocks. Proceedings of the Apolo 11 Lunar Science Conference 1, 481–497.

Glavatskih, S.F., 1990. Native metals and intermetallic compounds in the exhalative products of the Great Tolbachinsky fissure eruption (Kamchatka). Doklady Akademii Nauk SSSR (Reports of USSR Academy of Sciences) 313, 433–437 (in Russian).

Grime, G.W., Dawson, M., Marsh, M., McArthur, I.C., Watt, F., 1991. The Oxford submicron nuclear microscopy facility. Nucl. Instrum. Meth. B54, 52–63.

Gurov, E.P., Kudinova, L.A., 1987. Native metals from the meteoritic crater El'gygytgyn. In: Novye dannye o mineralah (New data on the minerals). Nauka, Moscow, 133–136 (in Russian).

Hannington, M.D., Peter, J.M., Scott, S.D., 1986. Gold in seafloor polymetallic silfide deposits. Econ. Geol. 81, 1867–1883.

Hansen, M., Anderko, K., 1958. Constitution of binary alloys, vol. I and II. McGraw–Hill, New York.

Hosking, K.F.G., 1974. The native tin story. Geol. Soc. Malays. Newsl. 50, 6–11.

Humphris, S.E., Alt, J.C., Teagle, D.A.H., Honnorez, J.J., 1998. Geochemical changes during hydrothermal alteration of basement in the stockwork beneath the active TAG hydrothermal mound. Herzig, P.M., Humphris, S.E., Miller D.J., Zierenberg R.A. (Eds.). Proc. ODP, Sci. Results 158, 255–276.

Ippatyeva, I.S., 1981. Form of presence of accessory native metals in granitoids and volcanic rocks from Yudomo–Mayskii region. In: Kovalskii, V.V. (Ed.), Samorodnoe mineraloobrazovanie v magmaticheskom processe (Native mineral formation in the magmatic processes). Yakutsk, 95–98 (in Russian).

Jedwab, J., Boulègue, J., 1984. Graphite crystals in hydrothermal vents. Nature 310, 41–43.

Jenkyns, H.C., 1976. Sediments and sedimentary history of the Manihiki Plateau, South Pacific Ocean. Initial reports of deep-sea drilling project, no. 33, Ocean Drilling Program, College Station, TX, pp. 873–890.

Johansson, S.A.E., Campbell, J.L, 1988. PIXE: A novel technique for elemental analysis. Wiley and Sons, Chichester.

Kovalskii, V.V. (Ed.), 1981. Samorodnoe mineraloobrazovanie v magmaticheskom processe (Native mineral formation in the magmatic processes). Yakutsk (in Russian).

Kovalskii, V.V., Oleynikov, O.B., 1985. Native metals and natural polymineral alloys of copper, zinc, lead, tin and antimony in the rocks of the kimberlite pipe 'Leningrad'. Doklady Akademii Nauk SSSR (Reports of USSR Academy of Sciences) 285, 203–208 (in Russian).

Kucha, H., 1981. Precious metal alloys and organic matter in the Zechstein copper deposits, Poland. TMPM Tschermaks Mineralogische und Petrographische Mitteilungen 28, 1–16.

Lawrence, L.J., 1951. Notes on an occurrence of native tin at Emmaville, N.S.W.. Aust. J. Sci. 13, 82–84.

Lazur, Y.M., Melamedov, S.V., Bernard, V.V., 1988. Native mineralisation in the Devonian volcanic–sedimentary deposits on the west slope of Middle Ural. Doklady Akademii Nauk SSSR (Reports of USSR Academy of Sciences) 298, 173–177 (in Russian).

Lazur, Y.M., Varentsov, I.M., Melamedov, S.V., Bernard, V.V., 1989. Dispersed Mn-, Fe-, Ti-, Cu-, and Zn-minerals in hydrothermal and pelagic sediments of the Galapagos Rift Zone. Chemie der Erde 49, 47–55.

Leinen, M., Rea, D.K., 1986. Shipboard Scientific Party, Site 597, Initial reports of the deep-sea drilling project, no. 92. US Government Printing Office, Washington, pp. 25–96.

Lisitsyn, A.P., 1972. Sedimentation in the World Ocean. Soc. Econ. Paleont. Mineral. Spec. Pub. 17.

Lisitsyn, A.P., (Ed.), 1992. Gidrotermal'naya deyatel'nost' v Sredinno-Atlanticheskom hrebte, gidrotermal'noe pole TAG: geologiya, geohimiya, processy rudoobrazovaniya (Hydrothermal activity on Mid-Atlantic Ridge (TAG field): geology, geochemistry, ore-forming processes). Nauka, Moscow (in Russian).

Lisitsyn, A.P., Bogdanov, Y.A., Zonenshain, L.P., Kuzmin, M.I.,, Sagalevitch, A, 1989. Hydrothermal phenomena in the Mid-Atlantic Ridge at latitude 26°N (TAG hydrothermal field). Int. Geol. Rev. 31, 1183–1198.

Marchig, V., Erzinger, J., Heinze, P.M., 1986. Sediment in the black smoker area of the East Pacific Rise (18.5ºS). Earth Planet. Sci. Lett. 79, 93–106.

Marcotte, V.C., Schroder, K., 1983. Cu–Pb–Sn ternary system: low Cu addition to Pb–Sn binary system. Mat. Res. Soc. Symp. Proc. 19, 403–410.

Mason, B., Melson, W., 1970. The lunar rocks. Wiley–Interscience, New York.

Maxwell, J.A., Teesdale, W.J., Campbell, J.L., 1995. The Guelph-PIXE software package-II. Nuclear Instruments and Methods B95, 407–421.

McGregor, B.A., Harrison, C.G.A., Lavelle, J.W., Rona, P.A., 1977. Magnetic anomaly patterns on Mid-Atlantic Ridge crest at 26°N. J. Geophys. Res. 82, 231–238.

Neumann, A., Richter, E., 1979. Tabellenbuch Schweiß- und Löttechnik. Wissensspeicher Schweiß-, Löt-, Kleb- und thermische Trenntechnik von Metallen und Plasten. VEB Verlag Technik, Berlin.

Novgorodova, M.I., 1994. Crystallochemistry of native metals and natural intermetallic compounds. Advancements of science and technology, Ser. Crystallochemistry 29, 3–150 (in Russian).

Okrugin, A.V., Oleynikov, B.V., Zayakina, N.V., Leskova, N.V., 1981. Native metals in the Siberian Platform traps. Zapiski Vsesoyuznogo Mineralogicheskogo Obshchestva (Reports of All-union Mineralogical Society) 110, 186–204 (in Russian).

Persikov, E.S., Buhtiyarov, P.G., Pol'skoy, S.F., Chehmir, A.S., 1986. Interaction of hydrogen with magmatic melts. In: Zharikov, V.A., Fed'kin, V.V. (Eds.), Eksperiment v reshenii geologicheskih zadach (experiment in solution of geological problems). Nauka, Moscow, pp. 48–70 (in Russian).

Prichard, H.M., Puchelt, H., Eckhardt, J.D., Fisher, P.C., 1996. Platinum-group-element concentrations in mafic and ultramafic lithologies drilled from Hess Deep. Proceedings of ocean drilling project, scientific results, no. 147, Ocean Drilling Program, College Station, TX, pp. 77–90.

Ramdohr, P., 1975. Die Erzmineralien und ihre Verwachsungen. Verlag, Berlin.

Rona, P.A., Hannington, M.D., Raman, C.V., Thompson, G., Tivey, M., Humphris, S.E., Labon, C., Petersen, S., 1993. Active and relict sea-floor hydrothermal mineralisation at the TAG hydrothermal field, Mid-Atlantic Ridge. Econ. Geol. 88, 1989–2017.

Rona, P.A., Klinkhammer, G., Nelsen, T.A., Trefry, J.H., Elderfield, H., 1986. Black smokers, massive sulfides, and vent biota at the Mid-Atlantic Ridge. Nature 321, 33–37.

Rona, P.A., Thompson, G., Mottl, M.J., Karson, J.A., Jenkins, W.J., Graham, D., Malette, M., Von Damm, K., Edmond, J.M., 1984. Hydrothermal activity at the TAG hydrothermal field, Mid-Atlantic Ridge crest at 26°N. J. Geophys. Res. 89, 11365–11377.

Rose, D., 1981. New data for stistaite and antimony-bearing η-Cu_6Sn_5 from Rio Tamaná, Colombia. Neues Jahrbuch für Mineralogie, Monahtchefte 3, 117–126.

Rudashevskii, N.S., Dmitrienko, G.G., Mochalov, A.G., Menshikov, Y.P., 1987. Native metals and carbides in the alpinotype ultramafites from Koryakskoe mountain. Mineralogicheskii Zhurnal (Journal of Mineralogy) 9, 71–82 (in Russian).

Sempéré, J.C., Purdy, G.M., Schouten, H., 1990. Segmentation of the Mid-Atlantic Ridge between 24°N and 30º40'N. Nature 344, 427–431.

Shterenberg, L.E., 1993. On the native metals on the Ocean floor. Mineralogicheskii Zhurnal (Journal of Mineralogy) 15, 79–85 (in Russian).

Shterenberg, L.E., Udintzev, G.B., Antipov, M.P., Voronin, B.I., Erih-Har, D.I., Korina, E.A., Sokolova, A.L., Kurentzova, N.A., 1993. Native metals in the basalts from San-Paulu fault zone (Atlantic Ocean). Byuletin Moskovskogo Obshchestva Ispytateley Prirody, seriya geologicheskaya (Bulletin of Moscow Association of the Explorers of Nature, Geological Section) 68, 101–107 (in Russian).

Silman, J.F.B., 1954. Native tin associated with pitchblende at Nesbitt LaBine uranium mines, Beaverlodge, Saskatchewan. Am. Mineral. 39, 529–531.

Stumpfl, E.F., Clark, A.M., 1965. Electron-probe microanalysis of gold–platinoid concentrates from southeast Borneo. Instn. Min. Metall. 74, 933–946.

Tomson, I.N., Polyakova, O.P., Polohov, V.P., 1989. Graphite–ilmenite mineralisation in tin deposits – an indicator of mantle gas jets (Primorie Region, USSR). Global Tectonics and Metallogeny 3, 101–106.

Zierenberg, R.A., Koski, R.A., Morton, J.L., Bouse, R.M., Shanks, W.C. III, 1993. Genesis of massive sulfide deposits on a sediment-covered spreading centre, Escanaba trough, southern Gorda Ridge. Econ. Geol. 88, 2069–2098.